

UCSF

UC San Francisco Previously Published Works

Title

Altered PBP4 and GdpP functions synergistically mediate MRSA-like high-level, broad-spectrum β -lactam resistance in *Staphylococcus aureus*.

Permalink

<https://escholarship.org/uc/item/2fs1c557>

Journal

mBio, 15(5)

Authors

Lai, Li-Yin

Satishkumar, Nidhi

Cardozo, Sasha

et al.

Publication Date

2024-05-08

DOI

10.1128/mbio.02889-23

Peer reviewed

Altered PBP4 and GdpP functions synergistically mediate MRSA-like high-level, broad-spectrum β -lactam resistance in *Staphylococcus aureus*

Li-Yin Lai,^{1,2} Nidhi Satishkumar,^{1,2} Sasha Cardozo,^{1,2} Vijay Hemmadi,^{1,2} Leonor B. Marques,³ Liusheng Huang,⁴ Sergio R. Filipe,^{3,5} Mariana G. Pinho,³ Henry F. Chambers,⁶ Som S. Chatterjee^{1,2}

AUTHOR AFFILIATIONS See affiliation list on p. 17.

ABSTRACT Infections caused by *Staphylococcus aureus* are a leading cause of mortality worldwide. *S. aureus* infections caused by methicillin-resistant *Staphylococcus aureus* (MRSA) are particularly difficult to treat due to their resistance to next-generation β -lactams (NGBs) such as methicillin, nafcillin, and oxacillin. Resistance to NGBs, which is alternatively known as broad-spectrum β -lactam resistance, is classically mediated by PBP2a, a penicillin-binding protein encoded by *mecA* (or *mecC*) in MRSA. Thus, presence of *mec* genes among *S. aureus* spp. serves as the predictor of resistance to NGBs and facilitates determination of the proper therapeutic strategy for a staphylococcal infection. Although far less appreciated, *mecA*-deficient *S. aureus* strains can also exhibit NGB resistance. These strains, which are collectively termed as methicillin-resistant lacking *mec* (MRLM), are currently being identified in increasing numbers among natural resistant isolates of *S. aureus*. The mechanism/s through which MRLMs produce resistance to NGBs remains unknown. In this study, we demonstrate that mutations that alter PBP4 and GdpP functions, which are often present among MRLMs, can synergistically mediate resistance to NGBs. Furthermore, our results unravel that this novel mechanism potentially enables MRLMs to produce resistance toward NGBs at levels comparable to those of MRSA. Our study provides a fresh new perspective about alternative mechanisms of NGB resistance, challenging our current overall understanding of high-level, broad-spectrum β -lactam resistance in *S. aureus*. It thus suggests reconsideration of the current approach toward diagnosis and treatment of β -lactam-resistant *S. aureus* infections.

IMPORTANCE In *Staphylococcus aureus*, high-level, broad-spectrum resistance to β -lactams such as methicillin, also referred to as methicillin resistance, is largely attributed to *mecA*. This study demonstrates that *S. aureus* strains that lack *mecA* but contain mutations that functionally alter PBP4 and GdpP can also mediate high-level, broad-spectrum resistance to β -lactams. Resistance brought about by the synergistic action of functionally altered PBP4 and GdpP was phenotypically comparable to that displayed by *mecA*, as seen by increased bacterial survival in the presence of β -lactams. An analysis of mutations detected in naturally isolated strains of *S. aureus* revealed that a significant proportion of them had similar *pbp4* and $\underline{G}GDEF$ domain protein containing phosphodiesterase (*gdpP*) mutations, making this study clinically significant. This study not only identifies important players of non-classical mechanisms of β -lactam resistance but also indicates reconsideration of current clinical diagnosis and treatment protocols of *S. aureus* infections.

KEYWORDS *gdpP*, *pbp4*, β -lactam resistance, methicillin-resistant lacking *mec* (MRLM)

Editor Robert A. Bonomo, Louis Stokes Veterans Affairs Medical Center, Cleveland, Ohio, USA

Address correspondence to Som S. Chatterjee, schatterjee@umaryland.edu.

Li-Yin Lai and Nidhi Satishkumar contributed equally to this article. Author order was determined both alphabetically and in order of increasing seniority.

The authors declare no conflict of interest.

See the funding table on p. 18.

Received 24 October 2023

Accepted 4 March 2024

Published 26 March 2024

Copyright © 2024 Lai et al. This is an open-access article distributed under the terms of the [Creative Commons Attribution 4.0 International license](https://creativecommons.org/licenses/by/4.0/).

Staphylococcus aureus is a Gram-positive bacterium that is a frequent colonizer of the human population. It is also an opportunistic pathogen with the potential to cause a range of infections including skin and soft tissue infections, bacteremia, osteomyelitis, and sepsis (1). Along with its pathogenicity, *S. aureus* is infamous for its ability to evade antibiotic treatment either in the form of drug resistance or tolerance (2, 3). The ability of *S. aureus* to cause pathogenic infections, coupled with its potential to evade the actions of antibiotics, makes it one of the leading causes of morbidity in the world (4). Due to their high safety and efficacy, β -lactams are one of the most successful and commonly prescribed classes of antibiotics for bacterial infections (5). β -Lactams target the bacterial cell wall by binding and inactivating a class of proteins involved in the cell wall synthesis and maintenance, known as penicillin-binding proteins (PBPs). One of the implications of inactivation of PBPs is the weakening of the bacterial cell wall and subsequent cell death (6). Resistance to β -lactams can classically occur either as narrow-spectrum resistance associated with BlaZ, a β -lactamase that hydrolyzes and inactivates the β -lactam ring of the drug (7), or as broad-spectrum resistance attributed to *mecA* (or *mecC*), a gene that encodes PBP2a, which has decreased affinity to β -lactams (8). While narrow-spectrum resistance is limited to early-generation drugs such as penicillin, broad-spectrum resistance renders the entire class of β -lactam drugs ineffective, including next-generation β -lactams (NGBs). This reduced affinity toward β -lactams enables bacteria to survive in the presence of antibiotics, providing high-level resistance in strains characterized as methicillin-resistant *Staphylococcus aureus* (MRSA) (9), which resulted in over 100,000 deaths in 2019 in the US alone (4). The subsequent development of ceftaroline, an advanced-generation NGB with a high affinity for PBP2a, has largely aided in combating *mecA*-associated β -lactam resistance (10).

NGB resistance can also be detected in *S. aureus* isolates that do not contain *mec* genes, referred to as methicillin-resistant lacking *mec* (MRLM) strains. MRLMs may also have borderline oxacillin-resistant *S. aureus* phenotype (β -lactamase hyperproduction) (11) or modified *S. aureus* phenotype (modifications in *pbps* resulting in decreased affinity to β -lactams) (12). Although first detected in the 1980s, the underlying mechanisms of resistance in MRLMs remain unknown (13). A recent spur in detection of natural MRLM isolates prompted efforts to map the basis of NGB resistance among MRLMs (14–16). These studies, which primarily employed whole-genome sequencing of MRLM isolates, identified mutations associated with *pbps* or *gdpP* in high frequencies.

Prior to these recent efforts, our group performed a series of laboratory passaging experiments with NGB sensitive strains of *S. aureus* that lacked *mecA* with the aim to determine non-classical mechanisms of β -lactam resistance that are independent of PBP2a or BlaZ (17–19). Passaging of strains in NGBs produced variants that displayed high-level, MRSA-like resistance. These resistant strains most prominently harbored mutations in *pbp4* (encodes for PBP4) and GGDEF domain protein containing phosphodiesterase (*gdpP*) (encodes for *gdpP*), suggesting that the mutations associated with these genes played an important role in facilitating high-level NGB resistance (20). Our subsequent findings demonstrated that through regulatory site and/or gene-associated mutations, PBP4 resulted in β -lactam resistance (20, 21). On the other hand, mutations associated with the catalytic domain of *gdpP*, a phosphodiesterase that cleaves the second messenger cyclic-di-AMP (CDA), led to increased amounts of CDA within the cell, suggesting that the mutations led to GdpP's loss of function (22). Further, the *gdpP* mutants evaded β -lactam treatment by drug tolerance, a phenomenon where bacteria can survive β -lactam challenges without resulting in a change in minimum inhibitory concentration (MIC) (22, 23). However, altered functioning of neither PBP4 nor GdpP on their own accounted for the high-level, broad-spectrum resistance to β -lactams that we reported previously among the laboratory-passaged NGB-resistant strains (17, 19).

In this study, we examined the combined effect of mutations associated with *pbp4* and *gdpP* on resistance by employing MIC assay, population analysis, and growth assay, along with determining their effect on tolerance by performing a tolerance disk (TD) test (24). Strains containing mutations associated with both *pbp4* and *gdpP* had

significantly increased survival when challenged with different NGBs such as nafcillin, oxacillin and ceftaroline, demonstrating high-level, broad-spectrum β -lactam resistance, suggesting a synergistic effect between the two mechanisms. This synergistic action on resistance provides an explanation for the high-level resistance seen in the aforementioned laboratory-passaged strains. These findings thus suggest that MRLM strains, by means of altering PBP4 and GdpP functions, can develop resistance to NGBs to the extent that is comparable to MRSA strains. *In vivo* studies performed with *Caenorhabditis elegans* demonstrated that alterations in PBP4 and GdpP allow for successful infection in the presence of β -lactams, thus also having the potential to lead to therapy failure.

MATERIALS AND METHODS

Bacterial strains

S. aureus strains were cultured in tryptic soy broth (TSB) (BD Biosciences, USA) media with aeration or on tryptic soy agar (BD Biosciences) plates at 37°C. Strains carrying the *pTX Δ* plasmids were grown in media containing 12.5-mg/L tetracycline. The strains used in this study are listed in Table S1.

Construction of mutants

Primers used in this study are listed in Table S2. Mutations in the SF8300ex strain were introduced through allelic replacement as previously described (25). Briefly, the 1-kb upstream and downstream regions of the target gene (*gdpP* or *pbp4*) were amplified, and splice-overlap extension PCR was performed. The PCR product was cloned into either the *pKOR1* plasmid (26) or *pJB38* plasmid (27), and the resultant plasmid was confirmed by sequencing (Eurofins Genomics, USA) before its transformation into RN4220, following which it was introduced into the recipient strain. Standard allelic replacement procedure was then carried out as previously described (26), and the obtained mutant was validated using PCR and/or Sanger sequencing.

MIC assay

MICs were determined by broth microdilution method as described previously (28). Briefly, 1×10^5 colony-forming unit (CFU) bacteria were incubated for 48 h at 37°C in 0.2-mL cation-adjusted Mueller-Hinton broth (BD Biosciences) containing increasing concentrations of antibiotic (0.25–256.0 mg/L for nafcillin and oxacillin, 0.25–4.0 mg/L for ceftaroline). MIC was recorded as the lowest concentration without growth at 48 h. MIC assay was performed twice in order to ensure reproducibility.

Population assay

Population assay was performed as previously described (28). Briefly, *S. aureus* strains were cultured in 3-mL TSB at 37°C overnight. A 10- μ L volume of serially diluted bacterial culture was spotted onto the prepared antibiotic-containing tryptic soy agar (TSA) plates and incubated at 37°C for 48 h. Plates were read and expressed as CFU per milliliter. Tetracycline (12.5 mg/L) was added to media and plates for the complemented strains carrying the *pTX Δ* plasmid. The population assay was performed twice to ensure reproducibility.

Growth curve assay

Growth assays were performed as previously described using Bioscreen C, an automated growth curve analysis system (Growth Curves USA) (29). Briefly, overnight cultures of bacteria were diluted to an OD_{600 nm} of 0.1 in TSB with or without antibiotics, and 200 μ L of the bacterial dilution was pipetted into each well of a Bioscreen C plate in triplicate. Growth curves were performed with continuous orbital shaking for a period of 12 h at 37°C. The data were then analyzed for OD_{600 nm} values at each time point for every

antibiotic concentration used. Growth assay was performed twice in triplicate to ensure reproducibility, except for ceftaroline, due to its cost and limited availability.

TD test

TD test was carried out as previously described with minor modifications (30). Briefly, overnight bacterial cultures were adjusted to $OD_{600\text{ nm}}$ of 0.1, and 100- μL bacteria were plated onto TSA plates. A 6-mm disk containing 1- μg nafcillin (or oxacillin) was placed in the bacterial lawn, and the plates were left to incubate at 37°C. After 18 h, the zone of inhibition for each plate was marked, and the antibiotic-containing disks were replaced with 4-mg glucose-containing disks. The plates were incubated at 37°C for another 2 days, following which tolerant colonies were enumerated. Colonies were counted as described in Fig. S5C, where the inner half of the zone of inhibition was annotated, and the colonies present within this region were counted as tolerant. TD test was performed twice to ensure reproducibility.

Immunoblotting

Overnight cultures of bacteria were subcultured in 50-mL flasks containing TSB such that the initial $OD_{600\text{ nm}}$ of the flasks was 0.1. The cells were cultured to $OD_{600\text{ nm}} = 1$, following which they were collected and resuspended in phosphate-buffered saline (PBS) containing CompleteMini protease inhibitor cocktail (Roche). The cells were mechanically lysed using the FastPrep (MP Biochemicals), and whole-cell lysates were obtained. The cell membrane fraction was isolated from the lysates by performing ultracentrifugation at $66,000 \times g$ for 1 h (Sorvall WX Ultra 80 Centrifuge, Thermo Fisher Scientific, USA). After resuspending the obtained pellet with PBS, protein estimation was carried out using the Pierce BCA Protein Assay kit (Thermo Fisher). The samples were separated by performing SDS-PAGE on a 10% gel, following which they were transferred onto a low-fluorescence polyvinylidene difluoride membrane (Millipore). Blocking was performed for 1 h (5% skimmed milk in Tris-buffered saline containing 0.5% Tween), and primary antibody staining was carried out overnight at 4°C (polyclonal anti-PBP2a, custom antibody from Thermo Fisher, 1:1,000 or polyclonal anti-sortase A, custom antibody from Thermo Fisher 1:1,000). Secondary antibody staining was performed using an anti-rabbit antibody (Azure anti-rabbit NIR700 or Azure anti-rabbit NIR800 at 1:20,000 dilution). The blots were imaged using the Azure C600 imager.

β -Lactamase assay

Nitrocefin discs (BD BBL Cefinase β -Lactamase Detection Discs) were placed onto TSA plates following which bacteria were streaked onto the discs using sterile toothpicks. The plates were incubated at 37°C for 30 min, following which the plates were observed for change of color. A color change to red was considered as β -lactamase positive.

Intracellular CDA measurement from bacteria

CDA measurement was carried out as previously described with a few modifications (22, 31). Briefly, bacterial cells were collected after 6 h of culture, washed, and lysed in $1 \times$ PBS containing 1-mM EDTA using a FastPrep-24 homogenizer (MP Biomedicals). Bacterial cytosolic fraction was collected upon centrifugation. Aliquots of 40- μL cytosolic samples were mixed with 10- μL internal standard (20-ng/mL tenofovir, a phosphate group containing compound that is negatively charged in solution, similar to CDA), and 10 μL of the resulting mixture was injected into a liquid chromatography-tandem mass spectrometer (LC-MS/MS) system. The LC-MS/MS system consisted of AB Sciex API 5000 tandem mass spectrometer, Shimadzu Prominence 20ADXR ultra-fast liquid chromatography pumps, and SIL-20ACXR autosampler. A Hypercarb analytical column (100 by 2.1 mm, 3 mm; Thermo Fisher Scientific) and mobile phases 100-mM ammonium acetate (buffer A, pH 9.8) and acetonitrile (buffer B) were used for separation. Electrospray ionization in negative ion mode as the ion source and multiple reactions

monitoring with ion pairs m/z 657/133 for CDA and m/z 286/133 for the internal standard were used for quantification. Calibration standards were prepared with synthetic CDA (Biolog) dissolved in the PBS containing 1-mM EDTA. The calibration range was 10–500 ng/mL with lower limit of quantification at 10 ng/mL.

Bocillin assay

Bocillin assay was performed as described in our previous study with modifications. Briefly, *S. aureus* strains were cultured in TSB, and cell density was adjusted to $OD_{600\text{ nm}} = 0.1$ in 50-mL cultures. Samples were collected when the bacterial cells reached an $OD_{600\text{ nm}}$ of 1. The lysates were labeled with 1- μ M Bocillin-FL (Thermo Fisher Scientific) at 35°C for 30 min, and the reaction was terminated by adding a sample buffer and boiling the samples for 10 min. Twenty micrograms of each sample was analyzed by 10% SDS-PAGE. The gel was scanned with Typhoon 9410 imager (Amersham/GE Healthcare) to visualize the penicillin-binding proteins on the gel.

Bacterial peptidoglycan purification and analysis

Muropeptide purification from *S. aureus* was performed as previously described (32, 33). Briefly, cells were harvested at the exponential phase ($OD_{600\text{ nm}}$ 0.8–0.9) and boiled in 4% SDS to inactivate cell wall-modifying enzymes, following which the SDS was removed by washing cells several times with water. Cells were then lysed mechanically using SpeedMill PLUS homogenizer, following which cell wall and subsequently peptidoglycan purification was performed as described previously (32, 33). Purified peptidoglycan was treated with mutanolysin to obtain muropeptides that were reduced with sodium borohydride in borate buffer and analyzed by reverse-phase high-performance liquid chromatography using a Waters Acquity CSH C18 column. Elution was performed using a gradient up to 80% acetonitrile (0.3 mL/min) for 28 min at 205 nm.

Caenorhabditis elegans killing assay

Infection of *C. elegans* DH26 was performed as described previously (29). Briefly, after age synchronization, 15 L4 young adult worms were incubated with 1.5×10^6 *S. aureus* in each well of a 96-well flat plate. Bacteria were added in 100- μ L liquid assay media (80% M9 buffer, 20% TSB, 10-mg/L cholesterol, and 7.5-mg/L nalidixic acid), following which nafcillin was added at the indicated concentrations. Infection studies were conducted at 26°C for 72 h, and the survival rate was recorded.

C. elegans gut CFU determination was performed as previously described (29, 34). Briefly, 100 μ L of M9 buffer containing 10-mM sodium azide and 100-mg/L gentamicin (hereinafter buffer 1) was transferred to 96-well plates. Worms were transferred to 1.5-mL microcentrifuge tubes and washed twice with 500- μ L buffer 1. After gentamicin treatment, worms were washed three times with M9 buffer containing 10-mM sodium azide (hereinafter buffer 2) to remove gentamicin. Worms were then suspended in 300- μ L buffer 2. The 50- μ L supernatant (without worms) was removed, and the remaining 250- μ L sample (with worms) was lysed by vortexing with 200 mg of zirconium beads for 2–5 min. The before-and-after lysis samples were plated on TSA plates and incubated at 37°C overnight. CFU determination was carried out the following day.

Hemolysis assay

Overnight cultures of bacterial strains were spotted onto TSA-blood plates (5% sheep blood) in increasing volumes (2, 5, and 10 μ L) as indicated and were incubated at 37°C overnight, following which the plate was stored at 4°C before recording the hemolysis pattern.

Statistical analysis

Statistical significance was analyzed using one-way analysis of variance or by two-tailed Student's *t*-test on GraphPad Prism software (version 8; La Jolla, CA, USA).

RESULTS

Mutations associated with *pbp4* and *gdpP* are detected in high frequencies among MRLM strains

Our previous studies targeted at identifying non-classical mechanisms of NGB resistance in *S. aureus* demonstrated that mutations associated with *pbp4* and *gdpP* occurred in high frequencies in strains lacking *mecA* when passaged in NGBs (17–19). Among the six NGB-passaged strains studied, *pbp4*-associated mutations were detected in five strains, whereas *gdpP*-associated mutations were detected in all strains (Fig. S1; File S1). The *pbp4*-associated mutations were either regulatory site associated, i.e., mutations located upstream of the *pbp4* start codon, and/or were missense mutations detected within the gene. *pbp4* regulatory site-associated mutations led to increased expression of PBP4, resulting in a highly cross-linked cell wall (25), while the missense mutations either led to an altered protein structure, which lowered drug affinity or led to increased thermal stability that resulted in resistance (35, 36). Mutations associated with *gdpP* led to partial or complete loss of its phosphodiesterase activity (referred to as loss-of-function mutations), causing an increase in CDA concentrations in bacteria that enabled cells to survive in high concentrations of β -lactams, a phenomenon commonly referred to as antibiotic tolerance (37).

Following the detection of mutations in laboratory-passaged strains, we performed a literature search to determine if mutations associated with *pbp4* and/or *gdpP* were also relevant in natural isolates of MRLM strains. Indeed, three independent studies aimed at characterizing mutations associated with MRLM isolates each reported the presence of similar mutations associated with *pbp4* and/or *gdpP* (14–16) (Fig. 1; Fig. S2, File S1). The criteria used by all three studies to classify an isolate as MRLM, namely, the absence of *mec* genes and phenotypic resistance to oxacillin (MIC >2 mg/L) and/or ceftiofuran (MIC >4 mg/L), were consistent. This allowed us to uniformly classify the isolates based on their mutations, predict their phenotypic manifestations and their subsequent effect on β -lactam resistance despite being reported in independent studies.

Of the isolates reported in these studies, a total of 155 MRLM isolates (83.78%) had mutations associated with both *pbp4* and *gdpP*, while a relatively smaller subset of isolates had mutations associated with only *pbp4* (8 isolates, 4.32%) or only *gdpP* (22 isolates, 11.89%) (Fig. 1A). *pbp4*-associated mutations were either regulatory site-associated (25 of 163, 15.33%), missense mutations, that resulted in amino acid substitutions in the *pbp4* gene (37 of 163, 22.69%), or detected as both, regulatory site and missense mutations (101 of 163, 61.96%) (Fig. 1B and C). A majority of *pbp4*-associated mutations were thus detected in both the regulatory site as well as the gene. Of the 177 (36.72%) isolates that possessed *gdpP* mutations, 65 were nonsense mutations, causing premature truncation of GdpP due to the introduction of a stop codon (Fig. 1D). Sixty-three isolates (35.59%) were INDELs resulting in frameshift mutations, while 49 isolates (27.68%) had missense mutations. Importantly, our analysis led to the observation that a large proportion of the mutations (128 out of 177) would result in loss of GdpP function due to premature truncation either upstream of its catalytic DHH/DHHA1 domains (33 isolates with non-sense mutations, 28 with INDELs) or within the DHH/DHHA1 domains (32 isolates with non-sense mutations, 35 with INDELs) (Fig. 1D and E). This indicated that a large portion of the isolates would display increased CDA concentration, as well as β -lactam tolerance, a phenotype that was observed previously among our resistant laboratory-passaged strains (22).

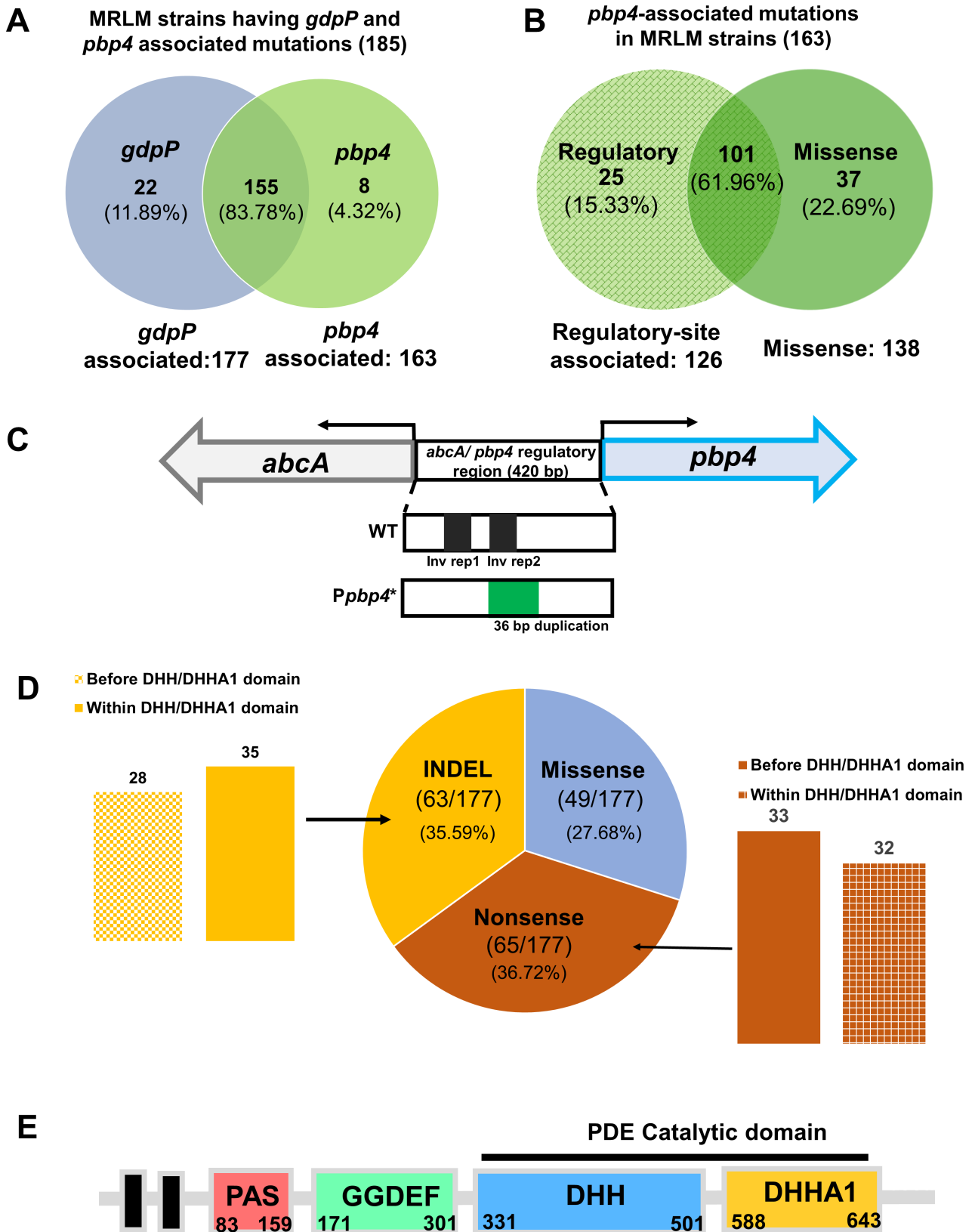


FIG 1 *GdpP* and *PBP4* mutations that were identified in MRLM isolates. (A) Venn diagram describing the occurrence of *pbp4* and/or *gdpP* mutations in MRLM strains described in previous studies. (B) Venn diagram describing the occurrence of *pbp4* regulatory site associated and/or missense mutations in MRLM strains described previously (C) Schematic diagram of *pbp4* and *abcA* genes separated by a 420-bp intergenic, regulatory site region for wild type (Wt) and the CRB (Continued on next page)

FIG 1 (Continued)

mutant. (D) Illustration and distribution of *gdpP*-associated mutations (insertion or deletion (INDELs), missense, and nonsense) detected in MRLM isolates. *gdpP*-associated mutations were further classified based on location of mutation with respect to the DHH/DHHA1 catalytic domain. (E) Schematic representation of different domains in the *gdpP* gene. The phosphodiesterase catalytic activity of GdpP is mediated by its DHH/DHHA1 domains.

Mutation-associated altered functions of PBP4 and GdpP synergistically produced high-level, broad-spectrum NGB resistance

Of the aforementioned laboratory-passaged strains, CRB was the strain where this unusual mode of resistance was initially identified (18). CRB contained mutations associated with *pbp4* (regulatory site and missense) and *gdpP* (loss of function) (17, 18). Unlike the other passaged strains, CRB did not have mutations associated with any other *pbps* and displayed high-level β -lactam resistance with a MIC of 256 mg/L for nafcillin (compared to a MIC of 1 mg/L for its susceptible parent), thus underscoring the potential roles of PBP4 and GdpP in high-level NGB resistance (17, 19). Further probing of the effect of *pbp4*-associated mutations was performed by introducing the regulatory site mutations (a 36-bp duplication 290 bp upstream the *pbp4* start codon) and missense mutations (E¹⁸³A and F²⁴¹R) detected in CRB into a NGB-sensitive parental strain. The presence of *pbp4*-associated mutations led to a considerable increase in resistance as seen by a MIC of 4 mg/L for nafcillin, when compared to its NGB-sensitive parental strain (20). While this increase in resistance was significant, it was not as high as that displayed by CRB, where the increase in MIC was 256-fold (17). CRB also contained loss-of-function mutations in *gdpP*. Loss-of-function mutations in *gdpP* did not result in a change in MIC but instead led to NGB tolerance (22). Taken together, *pbp4* and *gdpP* mutations resulted in broad-spectrum β -lactam resistance and tolerance, respectively; however, neither of them could independently produce the high-level resistant phenotype that was detected in CRB (17, 20). This led us to hypothesize that functional alterations of both PBP4 and GdpP are together required for high-level broad-spectrum β -lactam resistance. We thus sought to assess the effects of alterations in both PBP4 and GdpP by studying the effect of mutations detected in CRB (17, 18). The *pbp4* regulatory site (*Ppbp4**) and missense (*pbp4***) mutations were introduced in SF8300ex (Wtex): a *mecA* and *blaZ* excised wild-type (Wt) SF8300, a USA300, a prominent community-associated strain (Table S1; Fig. 2A) (2, 20, 29). Additionally, the loss-of-function effect of *gdpP* mutations was introduced by deletion of *gdpP*, thus resulting in the strain Wtex *Ppbp4** *pbp4*** Δ *gdpP* or the triple mutant. The resultant isogenic strains allowed us to assess the role of PBP4 and *gdpP* mutations together (Fig. 2A) in comparison to their parental strain (Wtex) as well as the wild-type MRSA strain (W).

At first, immunoblotting for PBP2a (76.1 kDa), the gene product of *mecA*, was carried out to verify the phenotypes of the obtained isogenic mutants. As expected, PBP2a was only detected in W (Fig. 2B), indicating that it was absent in all Wtex background strains. Further, a nitrocefin disk assay was performed to determine β -lactamase activity of the strains, which also confirmed that only the W strain contained BlaZ (Fig. 2C). The above tests thus verified that the studied mutants were devoid of the classical mediators of β -lactam resistance. Phenotypes associated with *pbp4* mutations were verified through Bocillin assay (Fig. 2D; Fig. S3). Strains with regulatory site mutations (*Ppbp4**) had an increased expression of PBP4 compared to all other strains. Alanine substitution of the essential active site serine of PBP4, S⁷⁵A, did not allow for Bocillin binding, and thus, no PBP4 bands were detected in the corresponding strains (Fig. 2D). Deletion of *gdpP* was verified by measuring levels of intracellular CDA; elevated levels of CDA were detected in strains that lacked *gdpP* compared to the other isogenic strains, confirming the Δ *gdpP* phenotype in these mutants (Fig. 2E).

Following the validation of strain phenotypes, we assessed their resistance profiles. MIC assay for *Ppbp4** *pbp4*** Δ *gdpP*, the triple mutant, revealed a drastic increase in resistance to nafcillin and oxacillin (64-fold), along with ceftaroline (8-fold) when compared to Wtex (Table 1). This increase in MIC values seen in the triple mutant

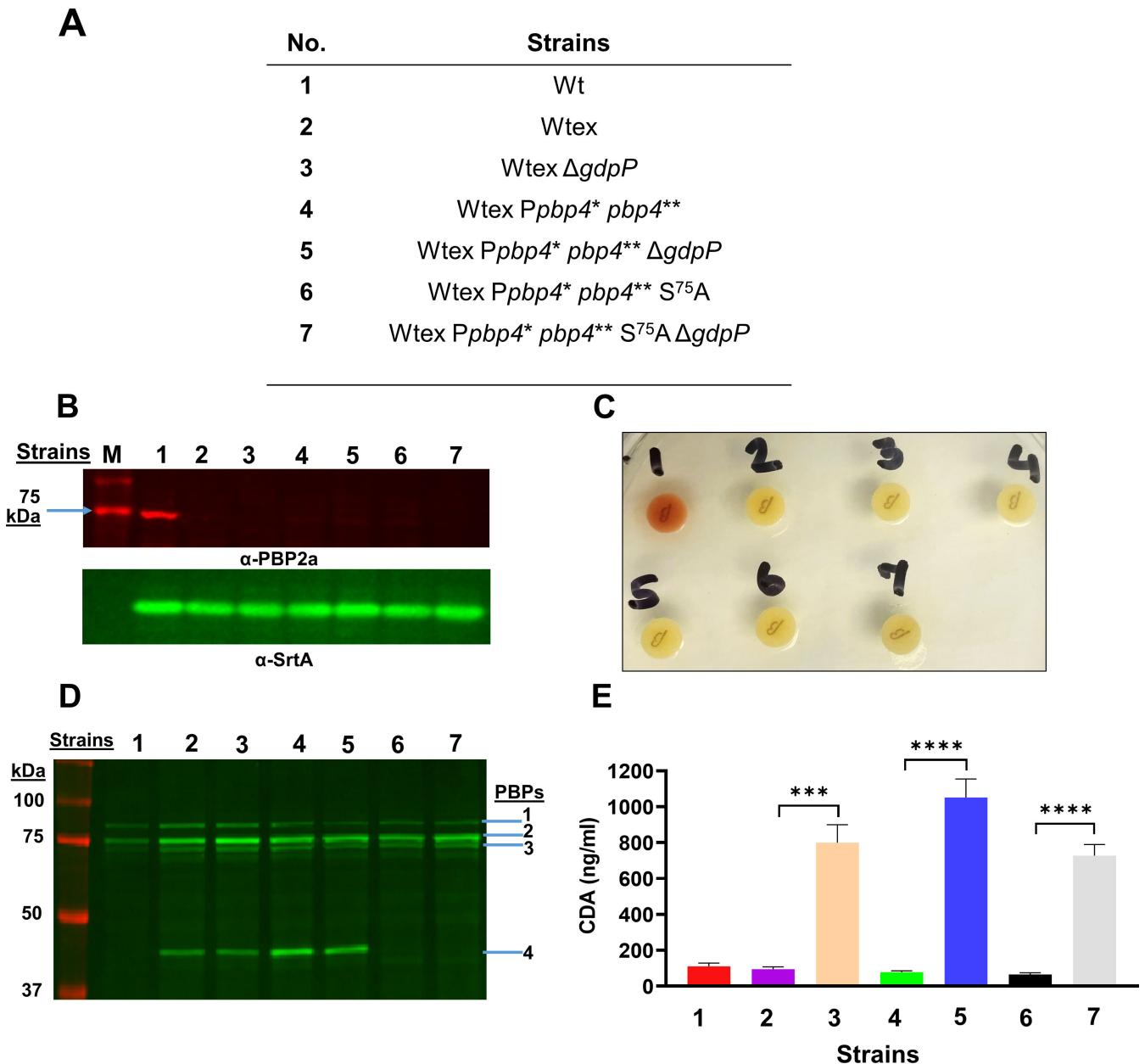


FIG 2 Phenotypic characterization of the strains used in this study. (A) List of strains used for obtaining the results for panels B–E. The regulatory site mutation (36-bp duplication, 36 bp upstream of the start codon) is represented as *Pbbp4**. Missense mutations (*E*¹⁸³*A* and *F*²⁴¹*R*) are represented as *pbp4***. (B) Immunoblotting with membrane fraction to detect PBP2a (α -PBP2a, 76.1 kDa, upper panel) was present in only lane 1 (W) and Sortase-A (α -SrtA, lower panel) as a loading control that was detected for all samples. “M” represents protein molecular weight marker. (C) Nitrocefin disk test indicated that only W had β -lactamase activity, as seen by the color change of the disk from yellow to red. The color of the disks streaked with other strains remained unchanged. (D) Bocillin assay with membrane fraction to detect PBP4 1–4. Strains with *pbp4* regulatory site mutations (lanes 4 and 5) showed enhanced PBP4 expression compared to the isogenic Wtex strain (lane 2). Strains with the *pbp4 S*⁷⁵*A* mutation (lanes 6 and 7) did not show any PBP4 band. Δ *gdpP* (lanes 5 and 7) did not have an effect on the expression of PBP4. PBP expression levels were visualized by the Typhoon 9410 imager (Amersham/GE Healthcare). (E) Measurement of intracellular levels of CDA for the studied strains. Strains with the Δ *gdpP* mutation show high levels of CDA compared to their isogenic pairs. $P = 0.0003$ for Wtex versus Wtex Δ *gdpP*; $P < 0.0001$ for Wtex *Pbbp4** *pbp4*** versus *Pbbp4** *pbp4*** Δ *gdpP*, and Wtex *Pbbp4** *pbp4*** *S*⁷⁵*A* versus Wtex *Pbbp4** *pbp4*** *S*⁷⁵*A* Δ *gdpP*. *** represents $P \leq 0.001$ and **** represents $P \leq 0.0001$.

was significantly higher than Wtex Δ *gdpP* as well as Wtex *Pbbp4** *pbp4***, suggesting a synergistic role of altered functions of PBP4 and GdpP (Table 1). Validation of this synergism was performed either by including the *pbp4* non-functional mutation,

TABLE 1 MIC assay of isogenic strains used in this study^a

No.	Strain	Notes (see Table S1 for more details)	Nafcillin (mg/L)	Oxacillin (mg/L)	Ceftaroline (mg/L)
1	Wt	<i>blaZ</i> and <i>mecA</i> positive USA300 strain	128.0	256.0	1.0
2	Wtex	Wt with <i>blaZ</i> and <i>mecA</i> excised	1.0	2.0	0.5
3	Wtex Δ <i>gdpP</i>	Wtex with <i>gdpP</i> deletion	1.0	4.0	0.5
4	Wtex <i>Ppbp4*</i> <i>pbp4**</i>	Wtex with <i>pbp4</i> regulatory and gene mutations	4.0	4.0	1.0
5	Wtex <i>Ppbp4*</i> <i>pbp4**</i> Δ <i>gdpP</i>	Wtex with <i>pbp4</i> regulatory, gene mutations, and <i>gdpP</i> deletion	64.0	128.0	4.0
6	Wtex <i>Ppbp4*</i> <i>pbp4**</i> <i>S</i> ⁷⁵ <i>A</i>	Strain 4 with inactivated PBP4 due to <i>S</i> ⁷⁵ <i>A</i> substitution	0.5	0.5	0.25
7	Wtex <i>Ppbp4*</i> <i>pbp4**</i> <i>S</i> ⁷⁵ <i>A</i> Δ <i>gdpP</i>	Strain 5 with inactivated PBP4 due to <i>S</i> ⁷⁵ <i>A</i> substitution	0.25	0.5	0.25

^aClinical and Laboratory Standards Institute (CLSI) breakpoints, based on document CLSI M100-ED33:2023, 33rd edition. S, susceptible; R, resistant. Oxacillin and nafcillin: ≤ 1 μ g/mL S, ≥ 4 μ g/mL R; ceftaroline: ≤ 1 μ g/mL S, ≥ 8 μ g/mL R.

*S*⁷⁵*A*, in the triple mutant (Wtex *Ppbp4** *pbp4*** *S*⁷⁵*A* Δ *gdpP*) or by complementing it with a functional GdpP [Wtex *Ppbp4** *pbp4*** Δ *gdpP* (*gdpP*)], both of which resulted in susceptibility to the selected NGBs (Tables 1 and 2). Additionally, the increase in MIC for the triple mutant was comparable to the *mecA*-containing W strain, and in the case of ceftaroline, the MIC was fourfold higher than that of Wt. These findings thus demonstrated that alterations in PBP4 and GdpP could synergistically result in MRSA-like, high-level NGB resistance. Population assay validated these findings, as the triple mutant had significantly increased resistance to nafcillin and oxacillin compared to the parent strain, Wtex, and could form an increased number of colonies in high concentrations of β -lactams similar to W (Fig. 3A and B). In alignment with the MIC assay values, the triple mutant had an increased ability of forming colonies compared to Wtex Δ *gdpP* and Wtex *Ppbp4** *pbp4***, reiterating the synergistic actions of altered PBP4 and GdpP. The inclusion of the *S*⁷⁵*A* mutation in the triple mutant (Wtex *Ppbp4** *pbp4*** *S*⁷⁵*A* Δ *gdpP*) resulted in absolute susceptibility to nafcillin and oxacillin (Fig. 3). Similar resistant phenotypes were observed when a growth assay was performed; in the absence of NGBs, strains with Δ *gdpP* had a growth defect, a well-established phenotype associated with the mutation. However, W and Wtex *Ppbp4** *pbp4*** Δ *gdpP* were the only strains that survived in the presence of nafcillin and oxacillin (Fig. S4). Complementation with functional GdpP [Wtex *Ppbp4** *pbp4*** Δ *gdpP* (*GdpP*)] also led to susceptibility in a population analysis (Fig. 4A and B). GdpP complementation was phenotypically verified by measuring intracellular CDA levels, where the mutant complemented with a functional GdpP contained decreased amounts of CDA compared to the mutants complemented with an empty vector (E) (Fig. 4C). The high-level, MRSA-like resistance to various NGBs was thus attributed to a synergistic effect brought about by mutations in both *pbp4* and *gdpP*.

Alterations in PBP4 and GdpP functions lead to a synergistic increase in resistance but maintain independent phenotypes

Since PBP4 and GdpP alterations resulted in a synergistic NGB resistance, we explored the mechanisms that could result in this synergy and assessed whether either of the proteins imparted an influence over the functioning of the other. We first assessed whether the deletion of GdpP affected expression of *pbp4*, which in turn led to alterations in cell wall cross-linking and producing NGB resistance. Bocillin assay

TABLE 2 MIC assay of complemented strains

Strain	Notes (see Table S1 for more details)	Nafcillin (mg/L)	Oxacillin (mg/L)	Ceftaroline (mg/L)
Wtex <i>Ppbp4*</i> <i>pbp4**</i> (E)	Strain 4 of Table 1 complemented with empty vector	1	1	1
Wtex <i>Ppbp4*</i> <i>pbp4**</i> Δ <i>gdpP</i> (E)	Strain 5 of Table 1 complemented with empty vector	32	64	4
Wtex <i>Ppbp4*</i> <i>pbp4**</i> Δ <i>gdpP</i> (<i>gdpP</i>)	Strain 5 of Table 1 complemented with constitutively expressing <i>gdpP</i>	2	2	1

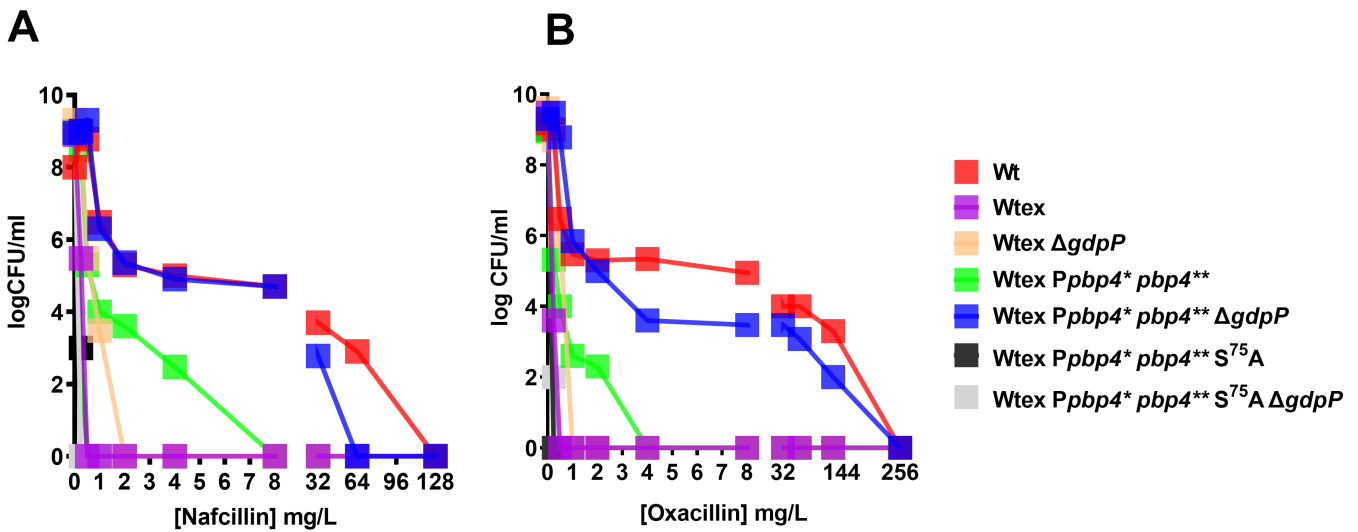


FIG 3 *pbp4* mutations and deletion of *gdpP* synergistically mediate high-level β -lactam resistance in *S. aureus*. Population analysis with (A) nafcillin and (B) oxacillin. The triple mutant, Wtex Pbp4* pbp4** $\Delta gdpP$ (blue squares), had increased survival compared to Wtex (pink squares), Wtex $\Delta gdpP$ (beige squares), and Wtex Pbp4* pbp4** (green squares). Resistance displayed by the triple mutant was comparable to that displayed by WT (red squares). Functional mutation of *pbp4* due to introduction of S⁷⁵A [Wtex Pbp4* pbp4** S⁷⁵A (black squares) and Wtex Pbp4* pbp4** S⁷⁵A $\Delta gdpP$ (gray squares)] resulted in NGB susceptibility.

demonstrated that the expression of PBP4, along with the other PBPs, remained unaffected by *gdpP* deletion, as there was no difference seen in PBP4 levels among Wtex and Wtex $\Delta gdpP$, or, Wtex Pbp4* pbp4** and Wtex Pbp4* pbp4** $\Delta gdpP$ strain pairs (Fig. 2D). Binding of Bocillin, a fluorescent analog of penicillin, to PBPs 1–4 was significantly diminished in W relative to Wtex background strains due to the presence of *blaZ*-encoded β -lactamase in W (Fig. 2D) as confirmed by the β -lactamase test (Fig. 2C). Since the deletion of *gdpP* did not affect expression levels of PBPs, we next characterized the cell wall profiles of the strains to determine whether the mutations brought about any changes to the cell wall composition (Fig. 5). In alignment with the observation that *gdpP* deletion had no effect on PBP4 expression as seen in the Bocillin assay, the deletion of *gdpP* also did not have an effect on the cell wall composition (Fig. 5A).

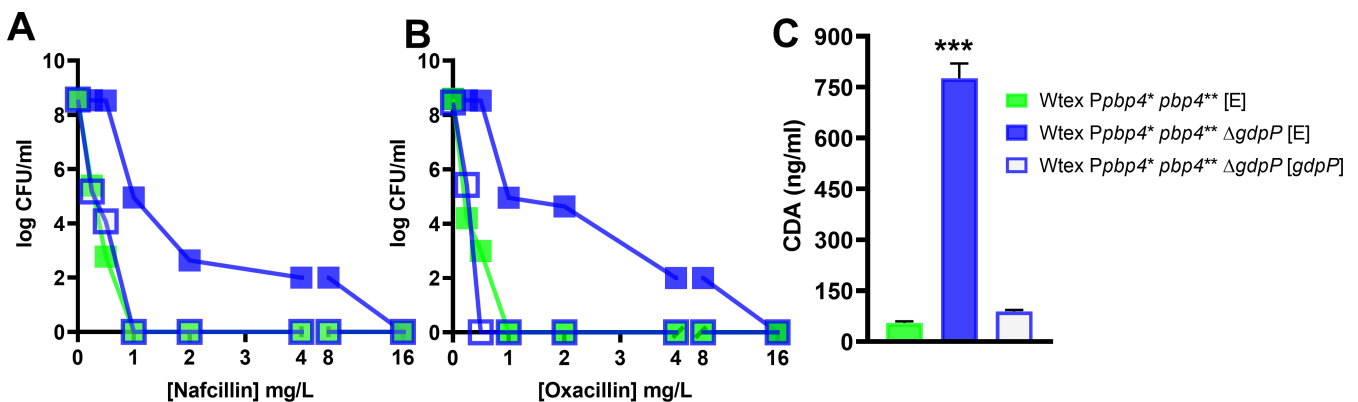


FIG 4 Complementation of *gdpP* restored β -lactam susceptibility of the NGB-resistant triple mutant. Population analysis of complemented strains carried out with (A) nafcillin and (B) oxacillin. Complementation of the triple mutant with a functional GdpP [Wtex Pbp4* pbp4** $\Delta gdpP$ (*gdpP*), empty blue squares] resulted in a loss of high-level resistance in a profile similar to Wtex Pbp4* pbp4** (E) (filled green squares). Complementation of the triple mutant with an empty vector [Wtex Pbp4* pbp4** $\Delta gdpP$ (E), filled blue squares] preserved the resistant phenotype associated with the mutations. (C) Measurement of intracellular levels of CDA for complemented strains. Complementation of the triple mutant with a functional GdpP [Wtex Pbp4* pbp4** $\Delta gdpP$ (*gdpP*), empty blue squares] led to decreased levels of CDA within cells that were similar to Wtex Pbp4* pbp4** (E) (filled green squares), whereas complementation of the triple mutant with an empty vector (Wtex Pbp4* pbp4** $\Delta gdpP$ (E), filled blue squares) maintained high levels of CDA.*** represents $P \leq 0.001$.

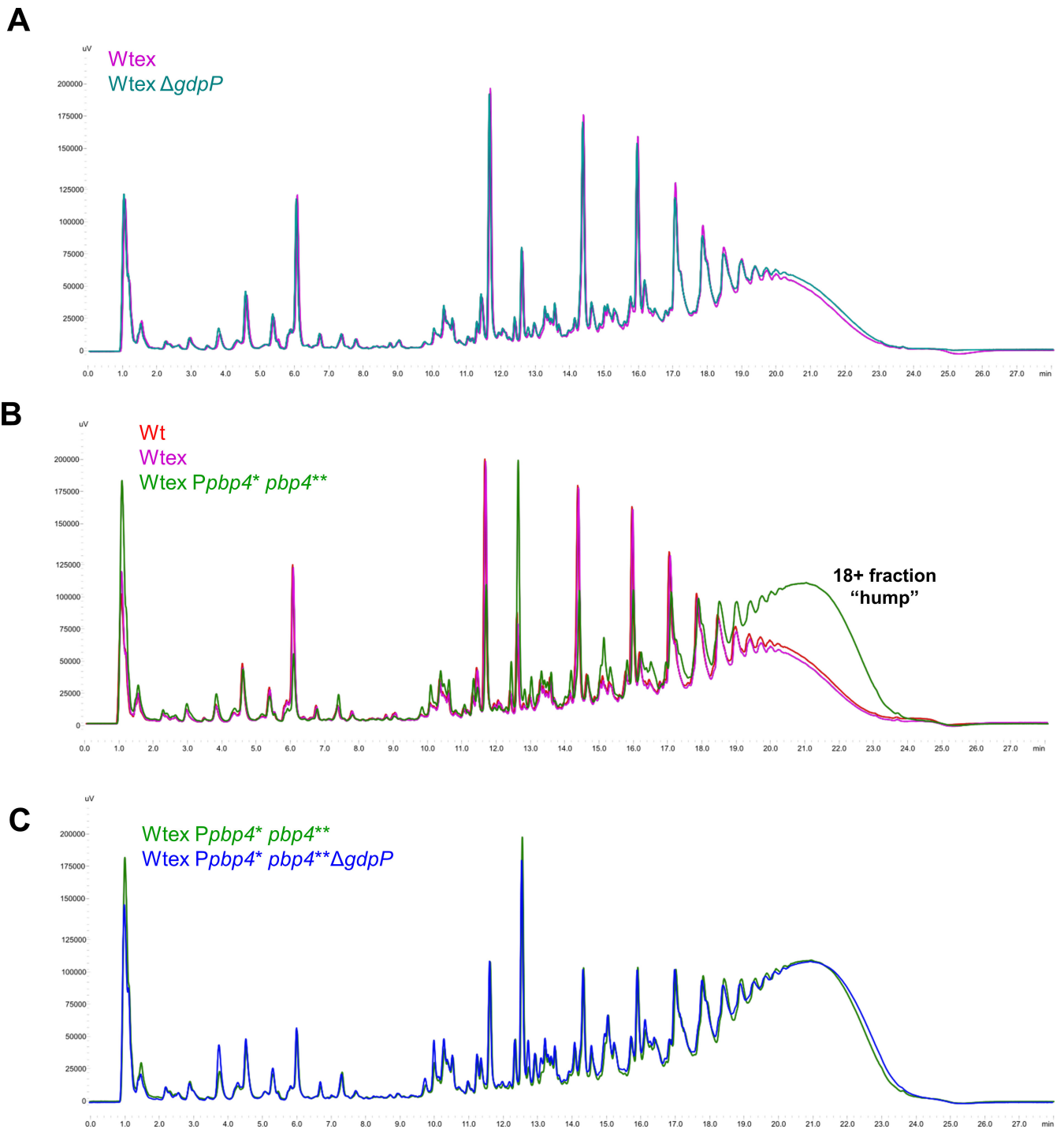


FIG 5 Alteration of GdpP does not affect the composition of the cell wall. Muropeptide purification and analysis profiles of (A) WT, Wtex, and Wtex *Pbp4** *pbp4***; (B) Wtex and Wtex $\Delta gdpP$; and (C) Wtex *Pbp4** *pbp4*** and Wtex *Pbp4** *pbp4*** $\Delta gdpP$. *pbp4*-associated mutations led to increased cell wall cross-linking (increased levels of peak 12 and peak 18+, i.e., the "hump") compared to Wtex. This increase was independent of $\Delta gdpP$. Similarly, deletion of *gdpP* did not contribute to any significant alterations in the cell wall, irrespective of the presence of *pbp4*-associated mutations.

There were no significant differences seen between the muropeptide profiles for W and Wtex, but the presence of *pbp4*-associated mutations, as seen previously (25), led to a significant increase in cell wall cross-linking as indicated by the increase in the 18+ muropeptide peaks or the "hump" (Fig. 5B). *pbp4*-associated increase in cell wall cross-linking remained unaltered in the presence of $\Delta gdpP$ in the triple mutant (Fig. 5C).

Taken together, these findings suggested that altered GdpP activity did not have any direct effect on the expression of PBPs or the peptidoglycan composition.

We next assessed if the *pbp4*-associated mutations affected the GdpP-induced tolerance phenotype. A hallmark of *gdpP* deletion and the subsequent elevation in intracellular levels of CDA is the ability of cells to exert tolerance toward β -lactams (22). To determine this, a TD test was performed (Fig. 6; Fig. S5) to measure the tolerance of each mutant to nafcillin (Fig. 6A and B) or oxacillin (Fig. 6C and D). TD tests involve treatment of bacteria with antibiotics (step I, Fig. S5), followed by exposure to glucose (step II, Fig. S5), to detect tolerant CFUs. Relatively similar amounts of CFUs were detected in both strains containing *gdpP* deletion (*P* value for *Wtex Δ gdpP* and *Wtex Ppbp4* pbp4** Δ gdpP* = 0.7779 for nafcillin and 0.2767 for oxacillin, not significant), suggesting that the presence of *pbp4*-associated mutations did not affect drug tolerance. Strains with an unaltered GdpP, namely, *Wtex* and *Wtex Ppbp4* pbp4***, did not generate any tolerant colonies, suggesting that tolerance was attributed only to the deletion of *gdpP* (Fig. 6A and C). These findings suggested that *pbp4*- and *gdpP*-associated mutations independently led to β -lactam resistance and tolerance, respectively, and alterations in their functions did not impart any influence on the other.

Synergistic action of PBP4 and GdpP alterations resulted in NGB therapy failure

To determine if synergistic action of altered functioning of PBP4 and GdpP, which brought about high-level resistance to NGBs *in vitro*, had an effect on bacterial survival during *in vivo* infection, we performed infection assays with *C. elegans* (Fig. 7A through

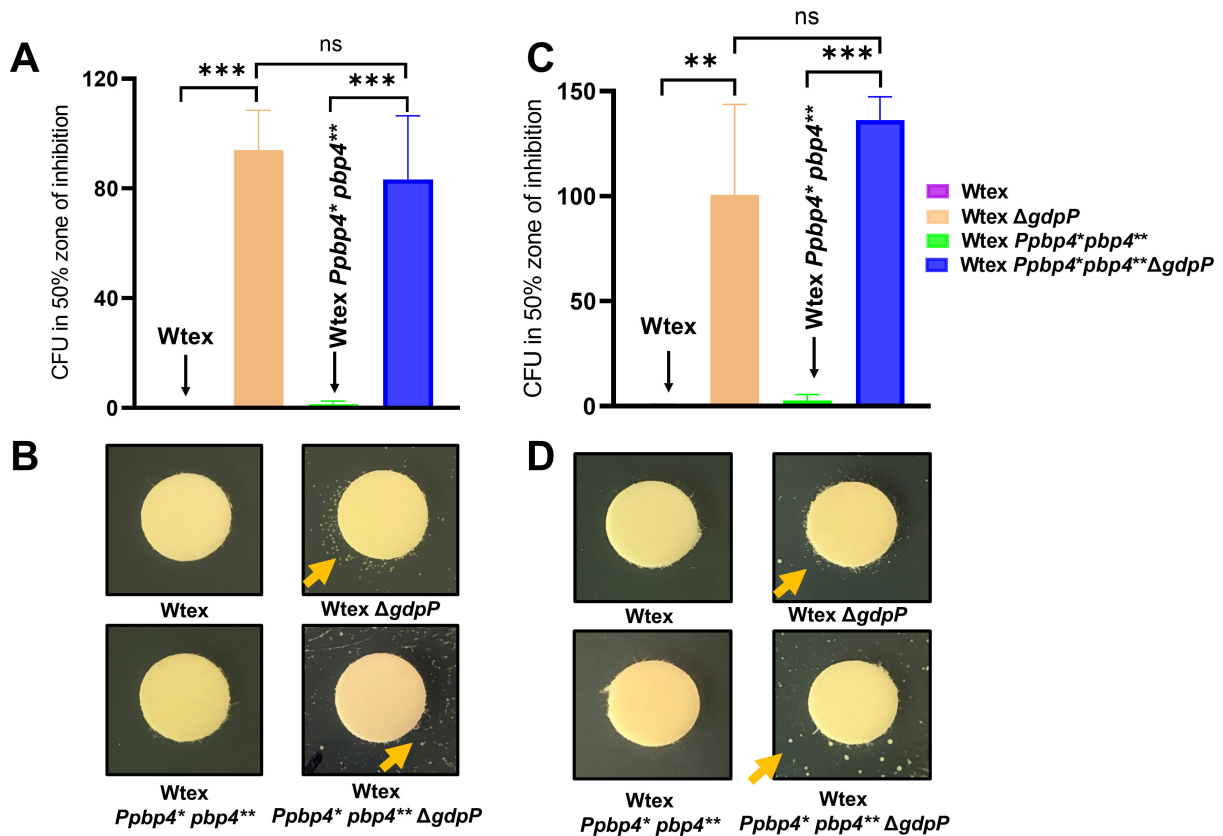


FIG 6 Deletion of *gdpP* led to NGB tolerance in *S. aureus*. TD test analysis to estimate tolerance levels in *S. aureus* strains. (A and B) TD test with nafcillin. (C and D) TD test with oxacillin. CFUs in the 50% inhibition zone of the strains containing *gdpP* deletion, namely *Wtex Δ gdpP* and *Wtex Ppbp4* pbp4** Δ gdpP* are higher compared to their isogenic strains with a functional GdpP, namely *Wtex* and *Wtex Ppbp4* pbp4***. All data are from three independent experiments and presented as mean \pm SD with one-way analysis of variance. ***P* \leq 0.01, ****P* \leq 0.001. ns, not significant.

D). Infection was performed with Wt, Wtex, or Wtex *Pbbp4** *pbbp4*** Δ *gdpP* in presence of increasing concentrations of nafcillin. While worms infected with Wtex had maximum survival, infection with Wtex *Pbbp4** *pbbp4*** Δ *gdpP* led to significant worm killing even in the presence of 4-mg/L nafcillin (80% worm survival) (Fig. 7A) or 8-mg/L nafcillin (85% worm survival), suggesting that the triple mutant maintained its resistant phenotype during *in vivo* infection (Fig. 7B). The worm survival was seen to be over 90% for all three strains only at the high concentration of nafcillin at 16 mg/L. (Fig. 7C). The killing pattern for the triple mutant was very similar to that displayed by W, which also resulted in killing of worms despite the presence of nafcillin (Fig. 7A and B), and required

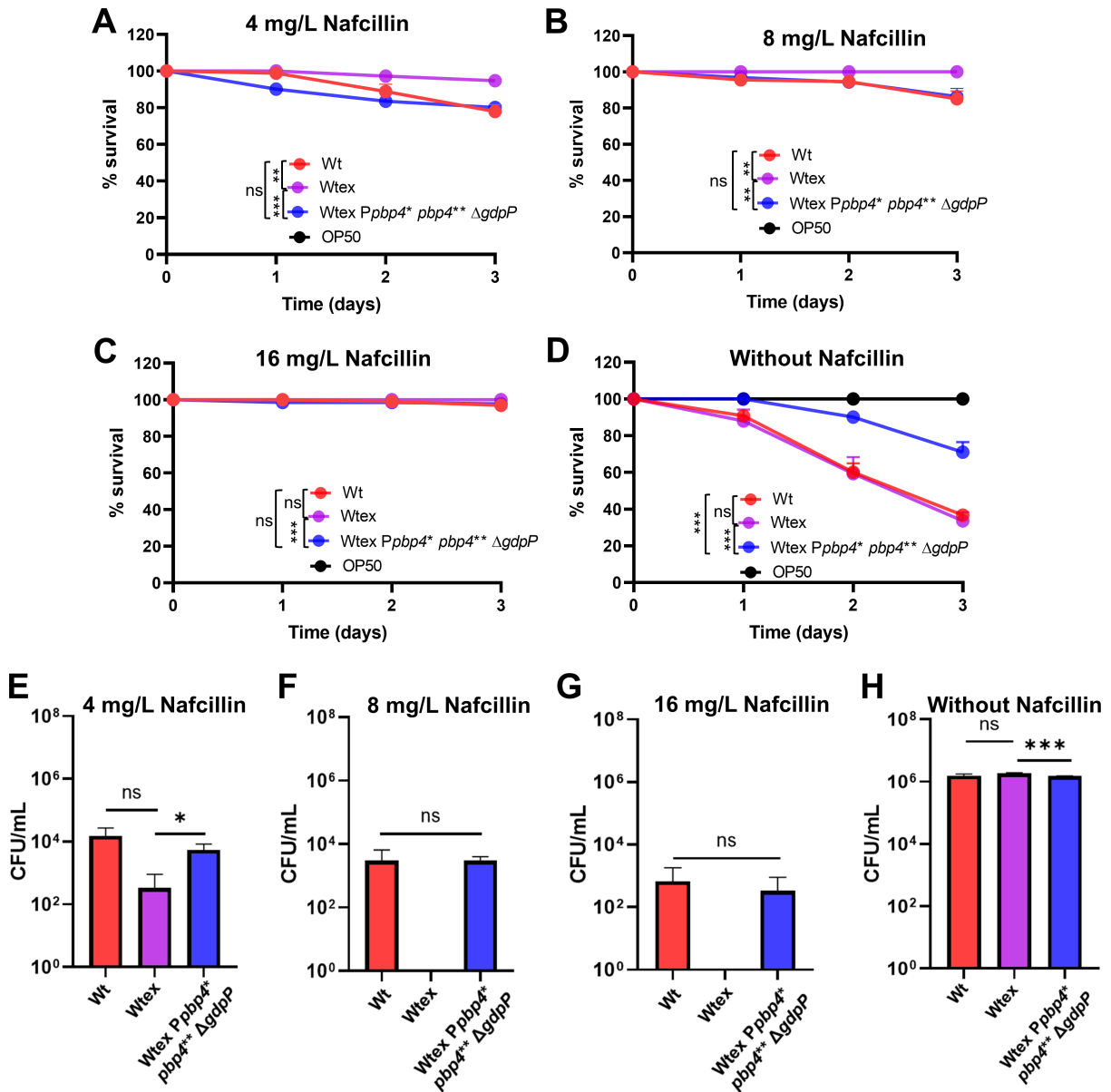


FIG 7 Synergistic action of PBP4 and GdpP alterations resulted in NGB therapy failure. Percent survival of *C. elegans* when infected with bacteria over a period of 72 h in the presence of (A) 4-mg/L, (B) 8-mg/L, or (C) 16-mg/L nafcillin. Worms infected with Wtex had 100% survival, whereas infection with Wtex *Pbbp4** *pbbp4*** Δ *gdpP* had decreased survival, similar to that seen by W. (D) The triple mutant, Wtex *Pbbp4** *pbbp4*** Δ *gdpP*, had attenuated virulence compared to Wt and Wtex the the absence of nafcillin. Worms infected with OP50, the *E. coli* control, showed 100% worm survival. Enumeration of bacterial load within the gut of *C. elegans* in the presence of (E) 4-mg/L, (F) 8-mg/L, or (G) 16-mg/L nafcillin. Compared to Wtex, which was not detected, W and Wtex *Pbbp4** *pbbp4*** Δ *gdpP* had significant colonization within the gut. (H) Gut bacterial enumeration when infection was carried out without nafcillin indicated that W, Wtex, and Wtex *Pbbp4** *pbbp4*** Δ *gdpP* had similar colonization abilities. * $P \leq 0.05$, ** $P \leq 0.01$, *** $P \leq 0.001$; ns denotes P value of >0.05 .

high concentrations of nafcillin in order to result in >90% worm survival (Fig. 7C), thus reiterating the MRSA-like resistance phenotype of the triple mutant. In the absence of antibiotics, W and Wtex strains led to maximum killing of the worms, resulting in 35% survival at the end of the 72-h assay. However, infection with the triple mutant led to a significantly higher worm survival of over 70%, suggesting an attenuation in virulence (Fig. 7D). OP50, the *Escherichia coli* control, maintained a 100% survival rate throughout the assay, indicating that the killing observed was attributed to *S. aureus* strains.

The bacterial load within the *C. elegans* gut was determined at the end of the assay by lysing the worms and enumerating CFUs (Fig. 7E through H). When infection was performed in the presence of nafcillin, CFU counts were the highest for Wt, followed by the triple mutant in a concentration-dependent manner, indicating that W and Wtex *Pbbp4* pbbp4** ΔgdpP* were successfully able to colonize *C. elegans* despite the presence of nafcillin (Fig. 7E through G). No CFUs were detected for Wtex, which was in alignment with 100% worm survival. In case of infection without nafcillin, there was no significant difference in CFUs among the strains, suggesting similar levels of bacterial colonization by each strain (Fig. 7H). Taken together, these findings demonstrated that the triple mutant, similar to Wt, could successfully colonize and kill *C. elegans* in the presence of nafcillin, suggesting that strains with alterations in PBP4 and GdpP have increased fitness during *in vivo* infection and can lead to therapy failure when treated with NGBs, in a manner similar to that seen by MRSA strains.

DISCUSSION

S. aureus is a frequent colonizer in humans and a major cause of infections associated with skin and soft tissue, lower respiratory tract, blood, or bones and joints (1, 38). Treatment of *S. aureus* can be challenging not only due to the nature of the infection that it causes, which ranges from bacteremia to biofilm formation, but also due to the ability of the pathogen to evade antibiotic treatment (2). Resistance to safe and effective antibiotics such as NGBs compels clinicians often to opt for alternatives that are known for having lower efficacy and adverse side effects (39). For the past several decades, *mecA* or *mecC* has been the hallmark of high-level NGB resistance in *S. aureus*, thus restricting the use of NGBs for treatment (8). However, NGBs (such as nafcillin and cefazolin) remain as the go-to drugs for treatment of infections caused by *S. aureus* strains that lack *mecA* (termed as MSSA), which are currently being detected in increasing numbers worldwide (5). Despite the lack of *mecA*, certain strains of MSSA can display NGB resistance and are termed as MRLMs, making the use of nafcillin or cefazolin ineffective. Following early identification in the 1980s, MRLMs have also been detected in recent years (14–16) (Fig. 1). MRLMs can be misdiagnosed as MSSA due to the lack of *mec* genes, which may cause improper therapeutic intervention, longer hospitalization, and increased healthcare-related cost. The underlying basis of MRLMs' resistance to NGB remained unknown. In this study, we demonstrated that mutations that alter PBP4 expression and function, along with mutations in *gdpP* that increase CDA production, can synergistically mediate NGB resistance (Fig. 3 and 8; Fig. S4). Abolition of either function of PBP4 (through S75A substitution at its active site) or reduction of CDA concentrations (through complementation with *gdpP*) produced total NGB susceptibility in the resistant strain. These results suggested that both PBP4 and CDA played an equally important role that caused NGB resistance in the resistant strain. To our surprise, NGB resistance in the triple mutant, *Pbbp4* pbbp4** ΔgdpP*, was not only significantly higher than its parental strain, Wtex, but also comparable to W, a MRSA strain. Notably, the triple mutant out-completed Wt when challenged with ceftaroline (a highly advanced NGB that is currently used to treat complicated MRSA infections) when assessed through MIC assay (Tables 1 and 2). To assess these results more objectively, we also performed growth curve analysis with ceftaroline, which produced results identical to those of MICs (Fig. 8). Thus, the synergistic mechanism of NGB resistance presented in this study not only identifies as at least one of the bases through which MRLMs could arise but also suggests that this mode of resistance is highly effective in producing

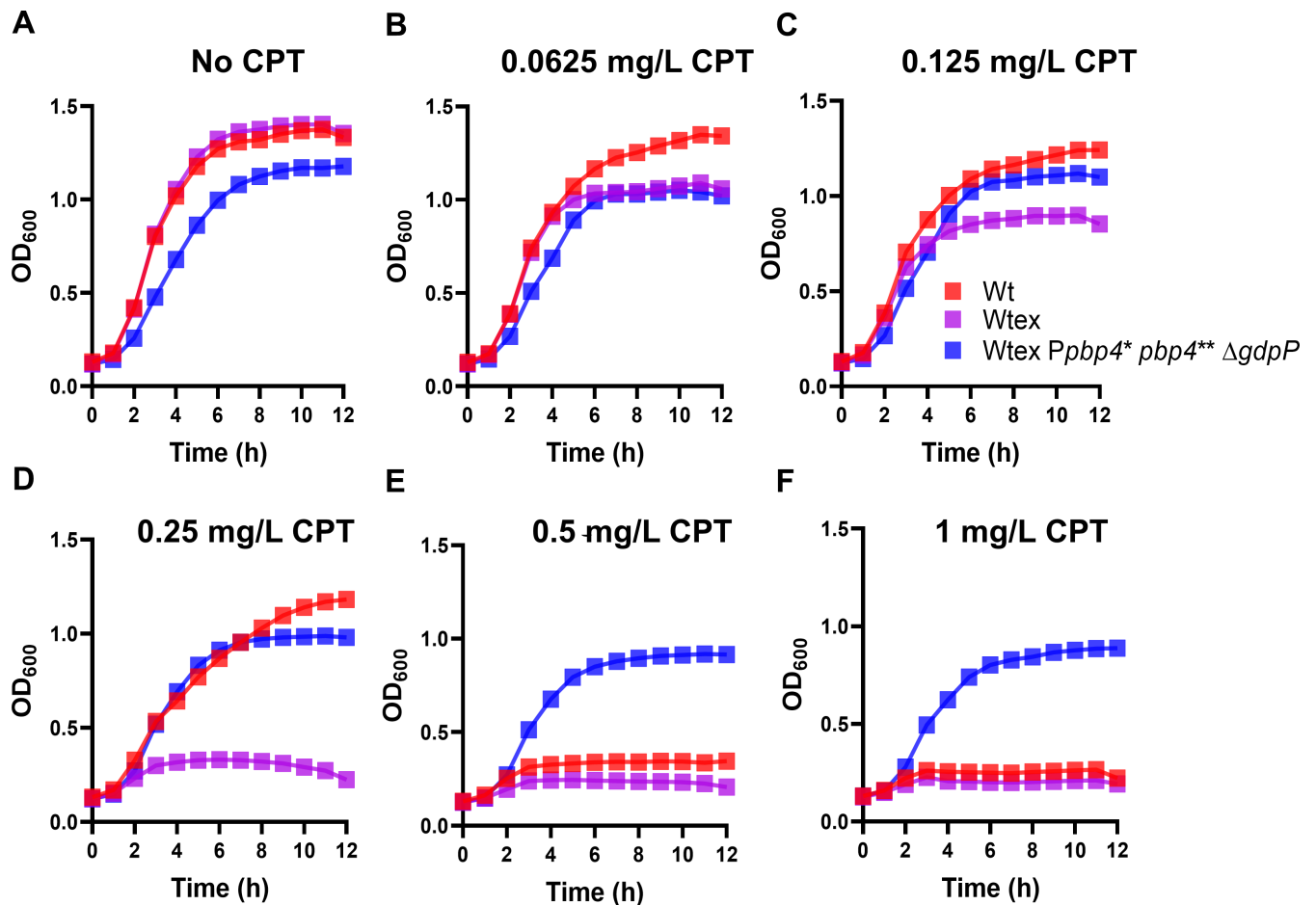


FIG 8 Growth assay in presence of ceftaroline. (A–F) Treatment of W, Wtex, and Wtex *Ppbp4** *pbp4*** Δ *gdpP* in increasing concentrations of ceftaroline (0–1 mg/L) demonstrated that W and Wtex were susceptible to ceftaroline. However, Wtex *Ppbp4** *pbp4*** Δ *gdpP* was not susceptible to the drug and survived even in the presence of the highest concentration of the drug.

NGB resistance that is typically observed in MRSA. Furthermore, the *in vivo* experiments demonstrated that, in the presence of Nafcillin, the NGB-resistant triple mutant was able to kill *C. elegans* at a significantly higher level compared to its NGB-susceptible parental strain (Fig. 7), indicating the possibility of therapy failure or an increase in therapeutic complications. Infection of *C. elegans* in the absence of drugs depicted a significant decrease in virulence of the triple mutant. This phenotype was consistent with previous studies demonstrating decreased *C. elegans* infection by strains possessing *pbp4*-associated mutations (29). Further, accumulation of intracellular CDA has also been previously associated with decreased virulence (40, 41). In line with our previously published results, strains with *gdpP* deletion, including the triple mutant, displayed decreased hemolysis when plated onto blood-agar plates, suggesting decreased virulence (Fig. S6) and reiterating that alterations associated with *pbp4* and *gdpP* alterations maintained their well-characterized, independent phenotypes in the triple mutant.

The results of our study also allude to a potential interaction between pathways involving PBP4 and GdpP that results in NGB resistance. PBP4 overexpression results in increased peptidoglycan cross-linking (25). We thus speculated if increased CDA levels led to an increase in the expression of PBPs that potentiated cell wall cross-linking. However, Bocillin assay and peptidoglycan analysis indicated that increased CDA neither had any effect on the expression of PBPs nor altered the cell wall profile, suggesting that there was likely no canonical change in the cell wall cross-linking in the triple mutant that facilitated the resistant phenotype (Fig. 2D and 5). Similarly, our results

also indicated that PBP4 overexpression did not influence tolerance to NGBs, a phenotype typically associated with increased CDA concentrations. Thus, the mechanism of synergism that brings about NGB resistance remains unclear at this point. We hypothesize that increased CDA concentrations influence PBP4 localization, stability, or turnover either in a direct or indirect manner to mediate high-level NGB resistance synergistically (Fig. S7). In bacteria including *S. aureus*, *Listeria monocytogenes*, and *Bacillus subtilis*, CDA has been associated with maintenance and stability of cell wall and β -lactam resistance (42–44). CDA also regulates the uptake of potassium ions by interacting with transporters such as KtrAB/AD and KdpFABC (45). In *Listeria monocytogenes*, CDA accumulation led to impaired activity of the D-alanine ligase, *ddl*, due to decreased uptake of potassium ions, resulting in decreased level of UDP-N-acetylmuramic acid and impaired peptidoglycan synthesis (46). However, such an alteration would have resulted in an altered muropeptide profile for the $\Delta gdpP$ strains (Fig. 5A). Conversely, in *Lactococcus lactis*, accumulation of CDA led to increased intracellular levels of UDP-N-acetylglucosamine, an integral component of the peptidoglycan (47, 48). Taken together, multiple studies have drawn associations between CDA and peptidoglycan synthesis, but it is evident that these associations are via intricate pathways and may vary between bacterial species. Thus, further studies are necessary to elucidate the role of CDA levels in peptidoglycan synthesis.

In summary, this study highlights that PBP4 and GdpP are together important players of NGB resistance and could have important roles in the development of MRLM strains, and should be further studied in order to uncover the mechanistic pathway leading to the synergistic, high-level NGB resistance.

Limitations

While we have attempted to identify the mechanism involved in this synergistic mode of NGB resistance, it remains unknown. Further studies include determination of the role of CDA in peptidoglycan synthesis, if any, and determination of the exact pathway where PBP4 and CDA interact, either directly or indirectly (Fig. S7).

ACKNOWLEDGMENTS

The authors thank Dr. Nicholas Carbonetti for his feedback on this article.

Research reported in this publication was supported by the National Institute of Allergy and Infectious Diseases of the National Institutes of Health under award numbers R01AI165510 and 2R01AI100291 to SSC. The content is solely the responsibility of the authors and does not necessarily represent the official views of the National Institutes of Health.

S.S.C. acknowledges the University of Maryland, Baltimore, and the University of Maryland Center for Environmental Science for providing seed funds. N.S. received Student Enhancement Funds from the Institute of Marine and Environmental Technology that partially covered travel expenses to Portugal for performing the cell wall analysis. L.B.M. was funded by fellowship UI/BD/153384/2022 from Fundação para a Ciência e a Tecnologia.

AUTHOR AFFILIATIONS

¹Department of Microbial Pathogenesis, School of Dentistry, University of Maryland Baltimore, Baltimore, Maryland, USA

²Institute of Marine and Environmental Technology (IMET), Baltimore, Maryland, USA

³Instituto de Tecnologia Química e Biológica António Xavier, Universidade Nova de Lisboa, Oeiras, Portugal

⁴Department of Clinical Pharmacy, Drug Research Unit, University of California, San Francisco, California, USA

⁵UCIBIO-REQUIMTE, Departamento de Ciências da Vida, Faculdade de Ciências e Tecnologia, Universidade Nova de Lisboa, Caparica, Portugal

⁶Division of Infectious Diseases, School of Medicine, University of California San Francisco, San Francisco, California, USA

AUTHOR ORCIDs

Nidhi Satishkumar  <http://orcid.org/0000-0003-1290-1159>

Liusheng Huang  <http://orcid.org/0000-0003-2702-4486>

Mariana G. Pinho  <http://orcid.org/0000-0002-7132-8842>

Som S. Chatterjee  <http://orcid.org/0000-0002-7138-4449>

FUNDING

Funder	Grant(s)	Author(s)
National Institute of Allergy and Infectious Diseases	R01AI165510 & 2R01AI100291	Som S. Chatterjee

ADDITIONAL FILES

The following material is available [online](#).

Supplemental Material

File S1 (mBio02889-23-s0001.xlsx). Mutations in *pbp4* and *gdpP* detected in clinical strains.

Supplemental data (mBio02889-23-s0002.docx). Supplemental tables and figures.

REFERENCES

- Sakr A, Brégeon F, Mège J-L, Rolain J-M, Blin O. 2018. *Staphylococcus aureus* nasal colonization: an update on mechanisms, epidemiology, risk factors, and subsequent infections. *Front Microbiol* 9:2419. <https://doi.org/10.3389/fmicb.2018.02419>
- Chambers HF, Deleo FR. 2009. Waves of resistance: *Staphylococcus aureus* in the antibiotic era. *Nat Rev Microbiol* 7:629–641. <https://doi.org/10.1038/nrmicro2200>
- Bui LMG, Conlon BP, Kidd SP. 2017. Antibiotic tolerance and the alternative lifestyles of *Staphylococcus aureus*. *Essays Biochem* 61:71–79. <https://doi.org/10.1042/EBC20160061>
- Murray CJL, Ikuta KS, Sharara F, Swetschinski L, Robles Aguilar G, Gray A, Han C, Bisignano C, Rao P, Wool E. 2022. Global burden of bacterial antimicrobial resistance in 2019: a systematic analysis. *Lancet* 399:629–655. [https://doi.org/10.1016/S0140-6736\(21\)02724-0](https://doi.org/10.1016/S0140-6736(21)02724-0)
- Bush K, Bradford PA. 2016. β -lactams and β -lactamase inhibitors: an overview. *Cold Spring Harb Perspect Med* 6:a025247. <https://doi.org/10.1101/cshperspect.a025247>
- Macheboeuf P, Contreras-Martel C, Job V, Dideberg O, Dessen A. 2006. Penicillin binding proteins: key players in bacterial cell cycle and drug resistance processes. *FEMS Microbiol Rev* 30:673–691. <https://doi.org/10.1111/j.1574-6976.2006.00024.x>
- Dyke KG, Jevons MP, Parker MT. 1966. Penicillinase production and intrinsic resistance to penicillins in *Staphylococcus aureus*. *Lancet* 1:835–838. [https://doi.org/10.1016/S0140-6736\(66\)90182-6](https://doi.org/10.1016/S0140-6736(66)90182-6)
- Fishovitz J, Hermoso JA, Chang M, Mobashery S. 2014. Penicillin-binding protein 2a of methicillin-resistant *Staphylococcus aureus*. *IUBMB Life* 66:572–577. <https://doi.org/10.1002/iub.1289>
- Berger-Bächli B. 1999. Genetic basis of methicillin resistance in *Staphylococcus aureus*. *Cell Mol Life Sci* 56:764–770. <https://doi.org/10.1007/s000180050023>
- Steed ME, Rybak MJ. 2010. Ceftaroline: a new cephalosporin with activity against resistant Gram-positive pathogens. *Pharmacotherapy* 30:375–389. <https://doi.org/10.1592/phco.30.4.375>
- Hryniewicz MM, Garbacz K. 2017. Borderline oxacillin-resistant *Staphylococcus aureus* (BORSA) – a more common problem than expected? *J Med Microbiol* 66:1367–1373. <https://doi.org/10.1099/jmm.0.000585>
- Tomasz A, Drugeon HB, de Lencastre HM, Jabes D, McDougall L, Bille J. 1989. New mechanism for methicillin resistance in *Staphylococcus aureus*: clinical isolates that lack the PBP 2a gene and contain normal penicillin-binding proteins with modified penicillin-binding capacity. *Antimicrob Agents Chemother* 33:1869–1874. <https://doi.org/10.1128/AAC.33.4.424>
- Chambers HF, Archer G, Matsushashi M. 1989. Low-level methicillin resistance in strains of *Staphylococcus aureus*. *Antimicrob Agents Chemother* 33:424–428. <https://doi.org/10.1128/AAC.33.4.424>
- Argudín MA, Roisin S, Nienhaus L, Dodémont M, de Mendonça R, Nonhoff C, Deplano A, Denis O. 2018. Genetic diversity among *Staphylococcus aureus* isolates showing oxacillin and/or ceftoxitin resistance not linked to the presence of *mec* genes. *Antimicrob Agents Chemother* 62:e00091-18. <https://doi.org/10.1128/AAC.00091-18>
- Sommer A, Fuchs S, Layer F, Schaudinn C, Weber RE, Richard H, Erdmann MB, Laue M, Schuster CF, Werner G, Strommenger B. 2021. Mutations in the *gdpP* gene are a clinically relevant mechanism for β -lactam resistance in methicillin-resistant *Staphylococcus aureus* lacking *mec* determinants. *Microb Genom* 7. <https://doi.org/10.1099/mgen.0.000623>
- Ba X, Kalmar L, Hadjirin NF, Kerschner H, Apfalter P, Morgan FJ, Paterson GK, Girvan SL, Zhou R, Harrison EM, Holmes MA. 2019. Truncation of GdpP mediates β -lactam resistance in clinical isolates of *Staphylococcus aureus*. *J Antimicrob Chemother* 74:1182–1191. <https://doi.org/10.1093/jac/dkz013>
- Banerjee R, Gretes M, Harlem C, Basuino L, Chambers HF. 2010. A *mecA*-negative strain of methicillin-resistant *Staphylococcus aureus* with high-level β -lactam resistance contains mutations in three genes. *Antimicrob Agents Chemother* 54:4900–4902. <https://doi.org/10.1128/AAC.00594-10>
- Banerjee R, Gretes M, Basuino L, Strynadka N, Chambers HF. 2008. *In vitro* selection and characterization of ceftobiprole-resistant methicillin-resistant *Staphylococcus aureus*. *Antimicrob Agents Chemother* 52:2089–2096. <https://doi.org/10.1128/AAC.01403-07>
- Greninger AL, Chatterjee SS, Chan LC, Hamilton SM, Chambers HF, Chiu CY. 2016. Whole-genome sequencing of methicillin-resistant *Staphylococcus aureus* resistant to fifth-generation cephalosporins

- reveals potential non-*mecA* mechanisms of resistance. PLoS One 11:e0149541. <https://doi.org/10.1371/journal.pone.0149541>
20. Basuino L, Jousselin A, Alexander JAN, Strynadka NCJ, Pinho MG, Chambers HF, Chatterjee SS. 2018. PBP4 activity and its overexpression are necessary for PBP4-mediated high-level β -lactam resistance. J Antimicrob Chemother 73:1177–1180. <https://doi.org/10.1093/jac/dkx531>
 21. Chatterjee SS, Chen L, Gilbert A, da Costa TM, Nair V, Datta SK, Kreiswirth BN, Chambers HF. 2017. PBP4 mediates β -lactam resistance by altered function. Antimicrob Agents Chemother 61:e00932-17. <https://doi.org/10.1128/AAC.00932-17>
 22. Poon R, Basuino L, Satishkumar N, Chatterjee A, Mukkayyan N, Buggeln E, Huang L, Nair V, Argudin MA, Datta SK, Chambers HF, Chatterjee SS. 2022. Loss of GdpP function in *Staphylococcus aureus* leads to β -lactam tolerance and enhanced evolution of β -lactam resistance. Antimicrob Agents Chemother 66:e0143121. <https://doi.org/10.1128/AAC.01431-21>
 23. Griffiths JM, O'Neill AJ. 2012. Loss of function of the *gdpP* protein leads to joint β -lactam/glycopeptide tolerance in *Staphylococcus aureus*. Antimicrob Agents Chemother 56:579–581. <https://doi.org/10.1128/AAC.05148-11>
 24. Kotková H, Cabrnocová M, Lichá I, Tkadlec J, Fila L, Bartošová J, Melter O. 2019. Evaluation of TD test for analysis of persistence or tolerance in clinical isolates of *Staphylococcus aureus*. J Microbiol Methods 167:105705. <https://doi.org/10.1016/j.mimet.2019.105705>
 25. Hamilton SM, Alexander JAN, Choo EJ, Basuino L, da Costa TM, Severin A, Chung M, Aedo S, Strynadka NCJ, Tomasz A, Chatterjee SS, Chambers HF. 2017. High-level resistance of *Staphylococcus aureus* to β -lactam antibiotics mediated by penicillin-binding protein 4 (PBP4). Antimicrob Agents Chemother 61:e02727-16. <https://doi.org/10.1128/AAC.02727-16>
 26. Bae T, Schneewind O. 2006. Allelic replacement in *Staphylococcus aureus* with inducible counter-selection. Plasmid 55:58–63. <https://doi.org/10.1016/j.plasmid.2005.05.005>
 27. Bose JL, Fey PD, Bayles KW. 2013. Genetic tools to enhance the study of gene function and regulation in *Staphylococcus aureus*. Appl Environ Microbiol 79:2218–2224. <https://doi.org/10.1128/AEM.00136-13>
 28. Chan LC, Basuino L, Diep B, Hamilton S, Chatterjee SS, Chambers HF. 2015. Ceftriaxone- and ceftazidime-resistant methicillin-resistant *Staphylococcus aureus*. Antimicrob Agents Chemother 59:2960–2963. <https://doi.org/10.1128/AAC.05004-14>
 29. Satishkumar N, Lai LY, Mukkayyan N, Vogel BE, Chatterjee SS. 2022. A nonclassical mechanism of β -lactam resistance in methicillin-resistant *Staphylococcus aureus* and its effect on virulence. Microbiol Spectr 10:e0228422. <https://doi.org/10.1128/spectrum.02284-22>
 30. Gefen O, Chekol B, Strahilevitz J, Balaban NQ. 2017. TDtest: easy detection of bacterial tolerance and persistence in clinical isolates by a modified disk-diffusion assay. Sci Rep 7:41284. <https://doi.org/10.1038/srep41284>
 31. Burhenne H, Kaever V. 2013. Quantification of cyclic dinucleotides by reversed-phase LC-MS/MS. Methods Mol Biol 1016:27–37. https://doi.org/10.1007/978-1-62703-441-8_3
 32. Filipe SR, Tomasz A, Ligoxygakis P. 2005. Requirements of peptidoglycan structure that allow detection by the *Drosophila* toll pathway. EMBO Rep 6:327–333. <https://doi.org/10.1038/sj.embor.7400371>
 33. de Jonge BL, Chang YS, Gage D, Tomasz A. 1992. Peptidoglycan composition of a highly methicillin-resistant *Staphylococcus aureus* strain. The role of penicillin binding protein 2A. J Biol Chem 267:11248–11254. [https://doi.org/10.1016/S0021-9258\(19\)49903-1](https://doi.org/10.1016/S0021-9258(19)49903-1)
 34. Portal-Celhay C, Bradley ER, Blaser MJ. 2012. Control of intestinal bacterial proliferation in regulation of lifespan in *Caenorhabditis elegans*. BMC Microbiol 12:49. <https://doi.org/10.1186/1471-2180-12-49>
 35. Satishkumar N, Alexander JAN, Poon R, Buggeln E, Argudin MA, Strynadka NCJ, Chatterjee SS. 2021. PBP4-mediated β -lactam resistance among clinical strains of *Staphylococcus aureus*. J Antimicrob Chemother 76:2268–2272. <https://doi.org/10.1093/jac/dkab201>
 36. Alexander JAN, Chatterjee SS, Hamilton SM, Eltis LD, Chambers HF, Strynadka NCJ. 2018. Structural and kinetic analyses of penicillin-binding protein 4 (PBP4)-mediated antibiotic resistance in *Staphylococcus aureus*. J Biol Chem 293:19854–19865. <https://doi.org/10.1074/jbc.RA118.004952>
 37. Brauner A, Fridman O, Gefen O, Balaban NQ. 2016. Distinguishing between resistance, tolerance and persistence to antibiotic treatment. Nat Rev Microbiol 14:320–330. <https://doi.org/10.1038/nrmicro.2016.34>
 38. Tong SYC, Davis JS, Eichenberger E, Holland TL, Fowler VG. 2015. *Staphylococcus aureus* infections: epidemiology, pathophysiology, clinical manifestations, and management. Clin Microbiol Rev 28:603–661. <https://doi.org/10.1128/CMR.00134-14>
 39. Rodvold KA, McConeghy KW. 2014. Methicillin-resistant *Staphylococcus aureus* therapy: past, present, and future. Clin Infect Dis 58:S20–S27. <https://doi.org/10.1093/cid/cit614>
 40. Hu J, Zhang G, Liang L, Lei C, Sun X. 2020. Increased excess intracellular cyclic di-AMP levels impair growth and virulence of *Bacillus anthracis*. J Bacteriol 202:e00653-19. <https://doi.org/10.1128/JB.00653-19>
 41. Fahmi T, Port GC, Cho KH. 2017. c-di-AMP: an essential molecule in the signaling pathways that regulate the viability and virulence of Gram-positive bacteria. Genes (Basel) 8:197. <https://doi.org/10.3390/genes8080197>
 42. Whiteley AT, Garelis NE, Peterson BN, Choi PH, Tong L, Woodward JJ, Portnoy DA. 2017. c-di-AMP modulates *Listeria monocytogenes* central metabolism to regulate growth, antibiotic resistance and osmoregulation. Mol Microbiol 104:212–233. <https://doi.org/10.1111/mmi.13622>
 43. Luo Y, Helmman JD. 2012. Analysis of the role of *Bacillus subtilis* σ^m in β -lactam resistance reveals an essential role for c-di-AMP in peptidoglycan homeostasis. Mol Microbiol 83:623–639. <https://doi.org/10.1111/j.1365-2958.2011.07953.x>
 44. Corrigan RM, Abbott JC, Burhenne H, Kaever V, Gründling A. 2011. c-di-AMP is a new second messenger in *Staphylococcus aureus* with a role in controlling cell size and envelope stress. PLoS Pathog 7:e1002217. <https://doi.org/10.1371/journal.ppat.1002217>
 45. Gundlach J, Krüger L, Herzberg C, Turdiev A, Poehlein A, Tascón I, Weiss M, Hertel D, Daniel R, Hänel I, Lee VT, Stülke J. 2019. Sustained sensing in potassium homeostasis: cyclic di-AMP controls potassium uptake by KimA at the levels of expression and activity. J Biol Chem 294:9605–9614. <https://doi.org/10.1074/jbc.RA119.008774>
 46. Massa SM, Sharma AD, Siletti C, Tu Z, Godfrey JJ, Gutheil WG, Huynh TN. 2020. c-di-AMP accumulation impairs muropeptide synthesis in *Listeria monocytogenes*. J Bacteriol 202:00307–00320. <https://doi.org/10.1128/JB.00307-20>
 47. Commichau FM, Gibhardt J, Halbedel S, Gundlach J, Stülke J. 2018. A delicate connection: c-di-AMP affects cell integrity by controlling osmolyte transport. Trends Microbiol 26:175–185. <https://doi.org/10.1016/j.tim.2017.09.003>
 48. Zhu Y, Pham TH, Nhiep THN, Vu NMT, Marcellin E, Chakraborti A, Wang Y, Waanders J, Lo R, Huston WM, Bansal N, Nielsen LK, Liang Z-X, Turner MS. 2016. Cyclic-di-AMP synthesis by the diadenylate cyclase CdaA is modulated by the peptidoglycan biosynthesis enzyme GlmM in *Lactococcus lactis*. Mol Microbiol 99:1015–1027. <https://doi.org/10.1111/mmi.13281>